Nuclear Operating Company

South Texas Project Electric Generating Station P.O. Box 289 Wadsworth, Texas 77483

December 28, 2003
NOC-AE-03001659
10CFR50.90

U. S. Nuclear Regulatory Commission
Attention: Document Control Desk
One White Flint North
11555 Rockville Pike
Rockville, MD 20852

South Texas Project
Unit 2
Docket No. STN 50-499
Supplement 3 to Proposed Emergency Change to Technical Specification 3.8.1.1 Note 12

Reference: 1. Letter from G. L. Parkey to NRC Document Control Desk dated December 27, 2003, "Proposed Emergency Change to Technical Specification 3.8.1.1 Note 12" (NOC-AE-03001657).

2. Letter from David Jaffe, NRC, to J. J. Sheppard, STPNOC, dated December 23, 2003, "South Texas Project, Unit 2 – Issuance of Amendment Concerning One-Time Allowed Outage Time Extension for No. 22 Emergency Diesel Generator (TAC No MC1616)"

In Reference 1, STPNOC submitted a proposed emergency amendment to the STP Unit 2 Operating License NPF-80 to extend the one-time allowed outage time (AOT) for Unit 2 Standby Diesel Generator (SDG) 22 from 21 days, approved in Reference 2, to 113 days to allow time to complete repair of the SDG.

This letter responds to a request for additional information regarding the critical crack size of the Standby Diesel Generator's master connecting rod due to high cycle fatigue and the proposed interval between NDE inspections.

If there are any questions regarding this response, please contact Mr. Steve Thomas at (361) 972-7162.

A001

I declare under penalty of perjury that the foregoing is true and correct.

Executed on December 28, 2003.
date

G. L. Parkey
Vice President,
Generation

jal/

Attachments:
1. Response to Request for Additional Information

cc:
(paper copy)

Bruce S. Mallett
Regional Administrator, Region IV
U. S. Nuclear Regulatory Commission
611 Ryan Plaza Drive, Suite 400
Arlington, Texas 76011-8064

U. S. Nuclear Regulatory Commission
Attention: Document Control Desk
One White Flint North
11555 Rockville Pike
Rockville, MD 20852

Richard A. Ratliff
Bureau of Radiation Control
Texas Department of Health
1100 West 49th Street
Austin, TX 78756-3189

Jeffrey Cruz
U. S. Nuclear Regulatory Commission
P. O. Box 289, Mail Code: MN116
Wadsworth, TX 77483

C. M. Canady
City of Austin
Electric Utility Department
721 Barton Springs Road
Austin, TX 78704

(electronic copy)

A. H. Gutterman, Esquire
Morgan, Lewis & Bockius LLP

L. D. Blaylock
City Public Service

David H. Jaffe
U. S. Nuclear Regulatory Commission

R. L. Balcom
Texas Genco, LP

A. Ramirez
City of Austin

C. A. Johnson
AEP Texas Central Company

Jon C. Wood
Matthews & Branscomb

ATTACHMENT 1

Response to Request for Additional Information

1. **Provide the critical crack size that the master connecting rod will fail due to high cycle fatigue. Give length & depth or aspect ratio.**

   Response:

   As shown in the attached photograph of the fracture surface (Figure 1), the critical crack size is about 7 inches in length by about 1 inch in depth (the thickness of the ligament). This determination is based on empirical data obtained from examination of the fracture face.

2. **Provide a calculation that demonstrates that the minimal detectable crack size will not grow to the critical crack size and fail due to high cycle fatigue during the proposed interval between NDE inspections. The calculation needs to account for the possibility that an accident can occur prior to the end of the inspection interval and that the diesel will perform its mission without failure. The calculation should describe the results, the assumptions and inputs and method used so that an independent reviewer can verify the conclusions.**

   Response:

   The requested calculation is presented in two parts. The first part is a classical Paris Law Equation analysis for the initial portion of crack propagation. The second part is an empirical assessment of the failure timeline.

   STPNOC has developed a substantial amount of analytical information from the analyses performed for a 1989 event involving fracture of the SDG 22 No. 4 connecting rod. A comparison of the 2003 event and the 1989 event is included in Appendix A to this attachment.

   Part 1 Discussion

   Understanding the failure mechanism and the timeline associated with crack initiation and subsequent crack propagation is important for two reasons:

   1. Unit 1 SDGs 11, 12, 13 and the other two Unit 2 SDGs 21 and 23 are not susceptible to the type of failure that occurred on SDG 22. This is based on the connecting rods being crack-free and that the operating hours place the connecting rods well beyond the longest reasonable incubation period plus the time required to grow a hypothetical crack to detectable size.

   2. For SDG 22, the shortest possible incubation time and the time required to propagate a crack to critical size is essential for establishing an inspection periodicity which precludes a similar failure on the rebuilt SDG 22.

In the unlikely event that fatigue cracking of a master connecting rod were to occur, that cracking will occur in the ligament between the connecting rod bearing bore and the articulating rod bushing bore. The ligament is 9 inches long axially and about 1 inch thick between the bores. The fatigue cracking mechanism proceeds in stages. The first stage is initiation during which submicroscopic atomic planar rearrangements and dislocation motion occurs. The second stage is initial propagation according to the Paris Law Equation, when an actual crack has formed with a cyclic stress intensity factor equal to or greater than the threshold cyclic stress intensity factor required to drive the crack front across the fracture surface. This regime of cracking assumes an unvarying cyclic stress distribution and is valid for crack growth covering up to about 20% of the final fracture area and is characterized by a rapidly increasing crack propagation rate, da/dN, as the crack length increases.

Testing of materials for fatigue resistance is traditionally done to evaluate the resistance to initiation of fatigue cracks on a featureless (polished) surface. Many decades of testing have demonstrated the concept of an endurance limit. The fatigue limit may be established for most steels between 2 and 10 million cycles (Reference 1 of this Attachment). Typically, if a test specimen has tested for 10^7 (ten million) cycles or more, it has been shown to be operating at a stress below the endurance stress. Figure 2 represents an example of a Stress Corrosion and Corrosion fatigue curve. Although 10^7 stress cycles is well accepted as the endurance limit, for this assessment assuming that initiation could occur up to twice the time, or 20 million cycles, adds additional margin.

This 4-stroke cycle Cooper-Bessemer KSV engine experiences one stress cycle every 2 rotations, and the peak stress occurs at Top Dead Center (TDC) at the end of the master rod exhaust stroke. This loading is all from the inertia of bringing the master rod and piston to a stop and reversing its direction of travel and is unrelated to the gas pressure loads which depend on engine power output. These diesel engines always run at 600 rpm, and thus accumulate fatigue cycles at 300 stress cycles per minute or 18000 cycles per hour, independent of engine load. Therefore, a crack can initiate and begin to grow up to 1100 hours of operation (which equates to 20 million cycles).

Once the initiation process has been completed, (i.e., a crack-like configuration with a cyclic stress intensity factor $\Delta K = 6.2$ ksi $\sqrt{in}$ has been developed) that crack will propagate continuously at a rate described by the Paris Law Equation,

$$da/dN = A(\Delta K)^P$$

where A is a coefficient and P is an exponent, both of which are determined experimentally for a given alloy and heat treatment.

The connecting rods for the Cooper KSV engines were produced to Cooper Energy Service Material Specification No. C-5B. The mechanical properties are those specified by ASTM-A521 for Class CG forgings. The material specification allowed for alloys other than AISI-41XX with specific chemistry limits on carbon and other elements. The #4 connecting rod which failed in 1989 was AISI 1050 steel (Figure 3), oil quenched and tempered to 197-241 Brinell, straightened and stress relieved at 1000°F. The #9 connecting rod was AISI 4140 steel (Figure 3A) similarly processed to meet the same Cooper specifications. Small changes in chemistry for similar steels do not affect fracture toughness significantly, provided the method of forming, heat treatment, and stress relief produce the same microstructure, yield strength and hardness, as is the case for these connecting rods. Therefore, fracture toughness properties for all connecting rods are expected to be nearly identical, since all the rods were produced to the same Cooper specifications for hardness and yield strength. Connecting rods used for the repair of SDG22 are "new" old stock manufactured to the same material specifications.

For the connecting rod material as used by Cooper-Bessemer, Battelle determined the coefficient $A = 9.77 \times 10^{-12}$, and the exponent $P = 4.12$ (Reference 2 of this Attachment). The Battelle Report was reviewed and found to be applicable to the current situation. The details of the experimental determination of the Paris Law Equation parameters and the threshold value for fatigue crack propagation are clearly and completely presented in that reference.

The Paris Law Equation will be valid near the origin of the fatigue crack, as long as the stress field is constant, that is, unchanged by the crack itself. This applies while the crack extends over less than 20% of the eventual final fracture surface, or is about 1 inch deep and 2 inches wide at the connecting rod bore surface. The cyclic stress intensity ΔK can be calculated for the 2003 event directly from the fracture surface. As the attached photographs (Figures 4 and 5) show the fatigue fracture surface is exceptionally well-preserved and has an excellent set of beach marks preserved on the surface. In fatigue, a beach mark indicates a temporary arrest point for the fatigue crack, usually when the machine is not operating. In the case of the number 9 master connecting rod from SDG 22, the beach marks are in essence a "calendar" engraved on the fracture surface. Groups of beach marks close together represent consecutive monthly 4-hour surveillance runs, and the single large gap between such groups of beach marks represents crack growth during a 24-hour 18-month surveillance run.

A photograph of the fracture surface (Figure 5) was used to measure the crack growth and the number of beach marks. The photograph has a ruler scale at the bottom of picture. The measured crack growth for one group of beach marks is about 3/16 inches. There are 13 beach marks in this length. Thus on average, the fatigue crack grew 0.014 inch between two successive beach marks. This region of beach marks is about ½ inch from the origin. Each of these equivalent beach marks was associated with a normal monthly surveillance run, and in the relevant time frame that run was just over 4 hours in duration. Thus the measured crack growth rate per stress cycle, da/dN, is about 0.2 x 10E-6 inches per cycle. The stress cycles are counted from the peak stresses when the master connecting rod is at TDC at the end of its exhaust stroke, 300 cycles per minute at 600 rpm.

As noted above, the February 27, 1990, Battelle report provided the coefficient for the Paris Law Equation for this material, based on tests of actual connecting rod steel. Using this equation and inserting da/dN = 0.2 x 10E-6 inches per cycle, the ΔK for the crack at that depth was computed to be 11.13 ksi $\sqrt{in}$. The ΔK's for other crack depths between 0.1 inch and 1 inch were computed using the standard fracture mechanics relationship between stress intensity factor K, stress σ, and crack depth a:

$$K = Y\sigma\sqrt{\pi a}$$

where Y is a coefficient that is unity for ideal geometric circumstances, and near a value of one but varying based on geometric details for specific cases.

For cyclic stress intensity factors for fatigue, the change in stress intensity factor ΔK is proportional to the change in stress $\Delta\sigma$ via the modified fracture mechanics equation:

$$\Delta K = Y\Delta\sigma\sqrt{\pi a}$$

The ratio of the square root of crack depth over 0.5 inch was computed for a given crack depth, and this ratio was multiplied times the ΔK at 0.5 inch crack depth to produce the value of ΔK for the desired crack depth. This process was calculated for every 0.005 inch of crack depth, and is shown on the attached spreadsheet (Table 1). This calculation also shows that ΔK does not reach the threshold value until the crack depth is about 0.155 inches. The Paris Law Equation is then used to compute the average crack extension rate, da/dN, for every 0.005 inch interval, and this is then converted to the number of cycles, and the number of hours, required to cover each 0.005 increase in crack depth. Finally, starting with the crack at threshold depth, the number of hours for each interval is summed to provide, on the spreadsheet, the cumulative hours for the crack to reach any given depth up to 1 inch.

Several lines are highlighted on the spreadsheet. The first is at a depth of 0.16 inches[1], the minimum detection limit for *in situ* NDE UT detection at STP. This depth will be reached after only 30 hours of crack propagation after initiation is complete. The next highlighted line is at a crack depth of ¼ inch (0.25 inch). The value of ΔK has increased to 7.9 ksi $\sqrt{in}$, and the crack has reached this depth after a total of 191 hours of growth post-initiation. The next ¼ inch of growth, to a depth of ½ inch (0.5 inch) requires another 140 hours of growth, indicating some

---

1 An ultrasonic testing (UT) calibration standard was prepared by machining a narrow Electric Discharge Machining (EDM) notch into the crankshaft bore of another connecting rod to simulate a crack in the region near the initiation site of the failed section on the number 9 connecting rod. To ensure the detectability of a crack in the vicinity of the initiation site, the simulated flaw was positioned behind the drilled oil passage at a location just past the direct line-of-sight horizon of the phased-array UT transducer. The UT calibration standard demonstrated the capability to repeatedly detect a crack 0.16 inches deep at this location. Larger flaws positioned further around the curvature of the crankshaft bore or located on the smaller radius of curvature articulating pin bore opposite the initiation site are possible and are more difficult to detect. However, the 0.16-inch simulated defect is conservatively much smaller than any crack which could hypothetically exist in the plane of the initiation site at this point in the operating history. Photographs of the calibration standard are provided in reference 2 of the cover letter.

acceleration of the crack growth rate. Another ½ inch of growth, to a depth of 1 inch, uses up just 68 hours, as the ΔK value has increased to 15.7 ksi √in.

At this point in the assessment, the response to the first issue can be determined. Below is a summary of STP diesel engine connecting rods hours of operation:

Unit 1		Unit 2	
SDG 11	1691 hours	SDG 21	1802 hours
SDG 12	1880 hours	SDG 22	2116 hours
SDG 13	2111 hours	SDG 23	1834 hours

Since the lowest operating hours on any engine connecting rod is 1691 hours, sufficient operating time has elapsed such that any defect or condition which could possibly develop into a crack has had sufficient time to initiate and grow to a detectable condition (1130 hours based on 20 million cycles to incubate and crack propagation per Paris Law). Since the inspections on SDGs 11, 12, 13, 21 and 23 have confirmed that no such cracks exist, the conclusion that the connecting rods are operating below the endurance limit has been demonstrated and that no such cracks could ever develop is supported.

Part 2 Discussion

Beyond a crack depth on the order of 1 inch, the third stage of crack propagation occurs with load redistribution along parallel load paths as the crack itself increases the compliance of the ligament, reducing the cyclic stress distribution acting on the crack. This effect modulates or decreases the rate of acceleration predicted by the Paris Law Equation alone and accounts for the long crack growth period experienced with these connecting rods. If the acceleration continued, complete separation of the connecting rod would occur in less than 450 hours of crack propagation. However, this is inconsistent with the experience in 1989 (634 hours) as well as the current failure (2116 hours). The explanation is that the forces imposed on the fracture surface drop off as the crack grows because there are significant alternate load paths to carry stresses around the affected area (load redistribution) as the compliance of the cracked region increases. Thus the crack growth acceleration decreases considerably as the crack grows, and the total propagation time is on the order of 600 to 1100 hours after crack initiation.

Employing an analytical fracture mechanics model to evaluate the behavior of the event past this point is considerably more complicated because ΔK is influenced by two opposing factors: (1) increasing crack size and (2) decreasing stress applied to the crack face. Calculations of crack growth rate and the critical crack size in the ligament between the bores of the Cooper-Bessemer KSV master connecting rod is not necessary because the two incidents that have been associated with the connecting rods, in 1989 and in 2003 yielded experimental verification that critical crack size is 7 inches long, through-wall. The ligament length in the axial dimension is 9 inches. The definition of critical crack size is standard definition from fracture mechanics, that is the size of crack for a given stress field, that raises the stress intensity K to a level equal to the critical stress intensity K_{IC} (the fracture toughness) of the material. This large critical crack size is due

principally to load redistribution around the ligaments as the crack enlarges and the compliance of the master connecting rod in the vicinity of the ligament increases. This drops the applied stresses considerably and keeps the stress intensity from reaching the critical stress intensity value until the growing fatigue crack is relatively large compared to the total fracture surface.

The direct measurement of the critical crack size in the 2003 event, with corroboration between 1989 and 2003 events, is much better than any calculated approximation, especially in light of the load distribution phenomenon.

There is confirmation of the identification of the sub-critical fatigue crack from the final critical fast fracture in the well-preserved fracture surface. The attached photographs show the excellent beach marks that identify the fatigue crack covering the majority of the fracture surface.

Figure 6 is the crack initiation and growth timeline for SDG 22 operating hours to failure. Therefore, in order to address the issue of establishing an inspection periodicity, which precludes a similar failure on the rebuilt SDG 22, the time for an assumed crack to grow to critical size is determined from the empirical data. The failure occurred following more than 2100 hours of accumulated engine operation. Subtracting the doubly conservative initiation time (1100 hours) and the time required to grow to detectable size (30 hours), the time for a crack to grow from just below the detectable size to critical size is 970 hours.

Since a detectable crack of a depth of 0.16 inches will take at least 970 hours to grow to critical size and cause connecting rod failure and in an emergency situation the diesel is required to provide 7 days (168 hrs) of continuous operation for plant safety (References 3, 4 and 5), the indicated inspection interval would be calculated by subtracting 168 from 970 hours. This shows that if the connecting rods are inspected every (970 – 168 = 802) hours, they will maintain at least 168 hours of run time available, even if called on just before the next scheduled inspection. Therefore, an inspection interval of about 800 hours is considered acceptable. Per reference 6, inspections will be performed every 500 hours.

References 7, 8, and 9 were used in preparation of this evaluation. Figure 7 is a schematic representation of NDE calibration mockup.

References:

1. Mark's Standard Handbook for Mechanical Engineers, Eighth Ed., p. 5-9
2. Report No. 341B7139 by Battelle, "Failure Analysis of the KSV-4_2A master Connecting Rod to Cooper Bessemer Reciprocating, Cooper Industries", February 27, 1990.
3. NRC Standard Review Plan 9.5.4
4. STP UFSAR Ch. 9.5.4
5. STP UFSAR Ch. 8.3.1.1.4.9
6. Letter from T. J. Jordan to NRC Document Control Desk dated December 20, 2003, "Revision to Proposed Emergency Change to Technical Specification 3.8.1.1" (NOC-AE-03001653)
7. Materials Technology Report, "Investigation of Diesel Generator Engine Connecting Rod Failure – South Texas Project Unit 2", dated December 13, 1989.
8. APTECH Report, "Significance of Over-drilled Oil Holes on Fatigue Life of the KSV-4-2A Connecting Rod in the Standby Diesel Engines at South Texas Project", dated March 1990.
9. Applied Mechanics Report (AM-1852-C-1A), "Finite Element Analysis of the KSV-4-2A Master Connecting Rod, by Cooper-Besemer Reciprocating Products, Division Cooper Industries, Inc."

APPENDIX A

Although failure of the #4 connecting rod on SDG 22 in 1989 was a high-cycle fatigue failure in the same general location as the 2003 failure, the initiating mechanism, and therefore the initial propagation of the crack, was entirely different. The failure in 1989 resulted from an over-drilled hole leaving behind a significant surface defect with a very high stress concentration factor. As part of that 1989 investigation, analytical modeling and laboratory testing by APTECH, Battelle, and Cooper-Bessemer (the "ABC" analyses) detailed the stresses and fatigue cracking potential in the subject ligament with a depth of understanding far exceeding the original design evaluation. The existence and availability of the ABC analyses shortened the time to analyze and understand the current situation by many weeks. These reports address two components of fatigue; initiation of a fatigue crack, and propagation of a fatigue crack.

The growth of the crack in the 1989 incident, even in the initial stages of crack propagation, with ΔK just in excess of the threshold value of 6.2 ksi $\sqrt{in.}$, was significantly influenced by the high stress concentration from the sharp-cornered geometry of the partially broken-through hole. This accelerated the slowest, most time-consuming portion of the crack growth, and shortened the total time to failure. In addition, due to the tearing within the hole and the high stress concentration factor, there was essentially no initiation period; that crack started growing almost from initial operation of the engine.

The 1989 fatigue crack also initiated at the oil hole complex within the ligament. The 2003 fatigue crack initiated away from the oil holes. Because the critical region of the between-bore ligament is stressed in bending, and not just uniform tension, the transverse oil hole across this thinnest section of the ligament is not a major concern. The stresses are highest on the surfaces of the ligament, and lowest at the neutral axis between the surfaces. The axial oil hole is centered on the neutral axis of the ligament and has little influence on the stresses that lead to possible crack initiation at the surfaces. The oil hole does, however, reduce the resistance to a crack growing transversely across the ligament. This helps explain why the 1989 failure, growing primarily along the transverse oil hole, apparently propagated more quickly than the 2003 crack propagated. The transverse oil hole was not a contributor to the 2003 event.

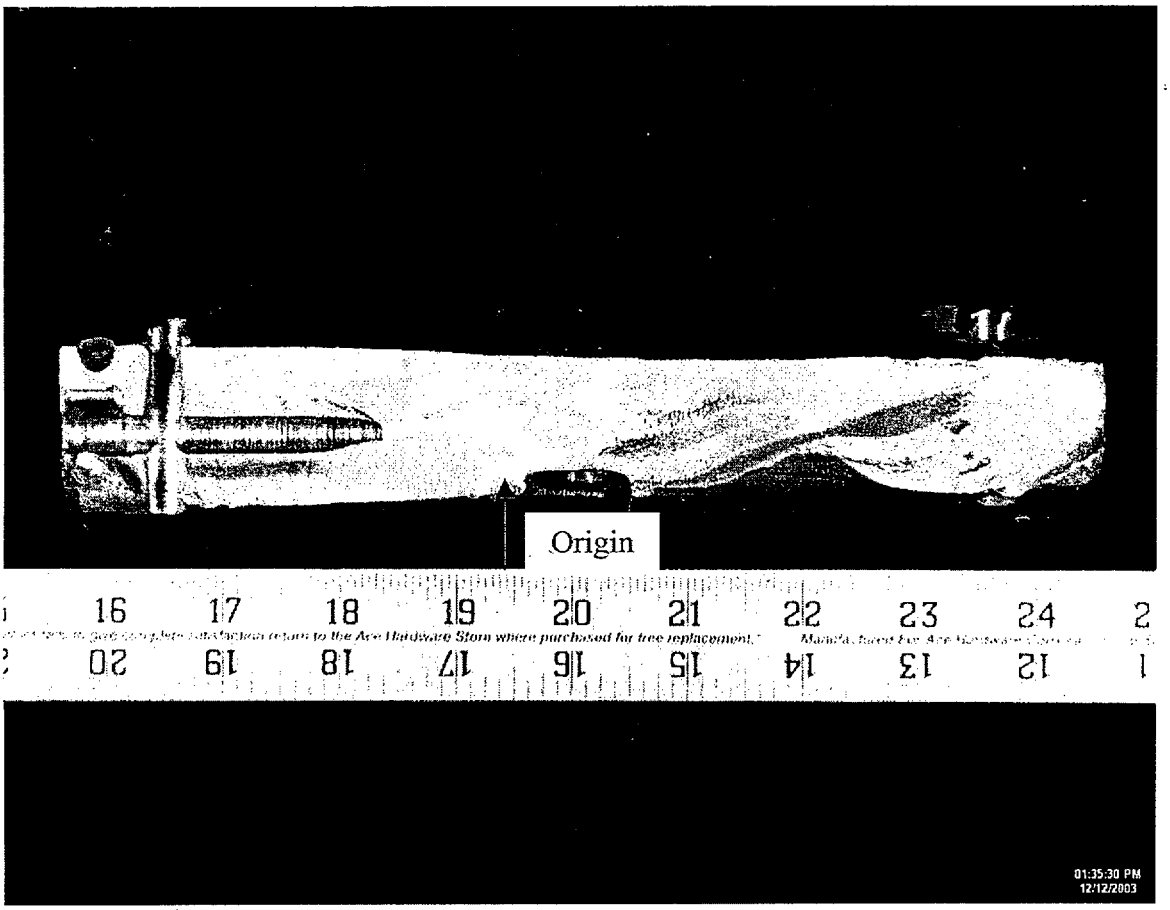

Figure 1
Photograph of the Fracture Surface

4140 Alloy Steel: Effect of Moisture and Dissolved Oxygen on Reversed Bending Fatigue Life, in Sodium Chloride

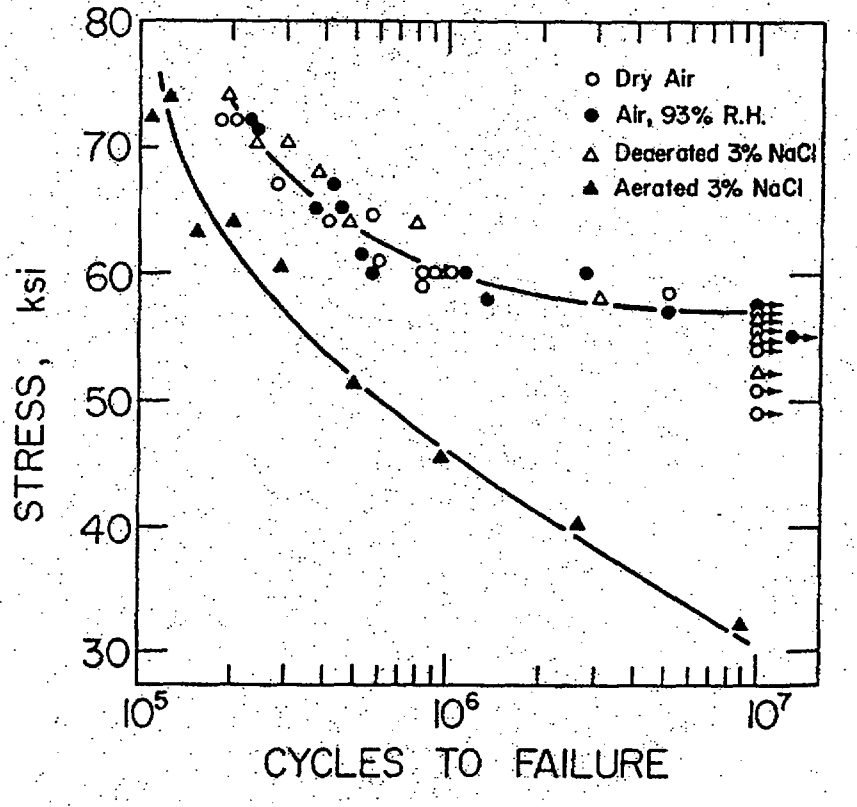

a)

Figure 2
Atlas of Stress Corrosion and Corrosion Fatigue Curves, (1990 Version) Edited by A. J. McEvily, Jr. - American Metals International, Page 106.

Cooper Energy Services
A Division of Cooper Industries
Mount Vernon, Ohio 43050
Attn: D. T. Wells (3)

FILE AP

(Chg 3)

Vendor: CANTON DROP FORGING & MFG. CO., Canton, Ohio

CERTIFICATION OF SHIPMENT

PART NO. KSV-4-2A NAME Rod & Cap

ECIFICATION C-5-D ORDER NO. 2621857U8 SHIPPING NOTICE 55501 DIE 0-4622

OCK SIZE 12" RCSq. ALLOY TYPE 1050 DATE SHIPPED 10/31/77 QUANTITY 35

MARKS: Oil quenched and tempered to 197-241 Brinell, straightened and stress relieved at 1000°F. Brinelled 100%.

MAT	Heat Number	Heat Code	Pcs.	Grain Size	C	Mn	P	S	Si	Ni	Cr	Mo	Cu	Al
epublic	6011354	R 14	35	FINE	.55	.75	.010	.035	.20	.10	.07	.01	.02	.0

SERIALS
CA-321 thru CA-355

HEAT	LOT	PHYSICAL PROPERTIES .2%YIELD (X1000)	ULTIMATE (X1000)	%RA	%ELONG.
6011354	10	66.3	108.8	58.1	26.6

MATERIAL CERTIFICATION
CONFORMS TO SPEC.
BY: [illegible] DATE: 12-22-77
NONCONFORMANCE:

MET LAB
APPVL BY: DATE:
TELE

ATE: November 4, 1977
bscribed and sworn to before me:

Caryn G. Smith
(Notary Public)

CARYN G. SMITH
Notary Public, State of Ohio
My Commission Expires August 8, 1

We certify to the Chemical Analysis and Physical Test as reported herein:

THE CANTON DROP FORGING & MFG. CO.

Signed: [signature]

Figure 3

Figure 3A

Cooper Bessemer Company

...ar Energy Services
...vision of Cooper Industries
...t Vernon, Ohio 43050
...: D. T. Wells (3)

Vendor: CANTON DROP FORGING & MFG. CO., Canton, Ohio

CERTIFICATION OF SHIPMENT

(Chg 3)

PART NO. KSV-4-2A .... NAME Rod & Cap ....

...TION C-5-B ..... ORDER NO. 3621ES789 .... SHIPPING NOTICE 55217 .... DIE 9-4072

...E 12" RCSq. ... ALLOY TYPE ..... 4140 .... DATE SHIPPED ... 10/3/77 ...... QUANTITY ... 7 ....

Oil quenched and tempered to 197-241 Brinell,
straightened and stress relieved at 1000°F.
Brinelled 100%.

Heat Number	Heat Code	Pcs.	Grain Size	C	Mn	P	S	Si	Ni	Cr	Mo	Cu
6073464	V 74	7	FINE	.39	.89	.015	.028	.21	.13	.98	.16	.12

MATERIAL CERTIFICATION
VERIFICATION TO ... C.
BY: BL DATE ...
...
MET LAB
APPVL ... DATE ...
TELE.

MADE WITH 4140 GRADE STEEL   MARKED WITH WHITE PAINT

SERIALS
CA314 thru CA320

...perties for Heat 6073464 Lot 7 were reported on 5/7/76, P.O. 3621-E-4600, P/S 5...

...,1977 ....

...re me:

We certify to the Chemical An...
as reported herein

NOC-AE-03001659
Attachment 1
Page 13

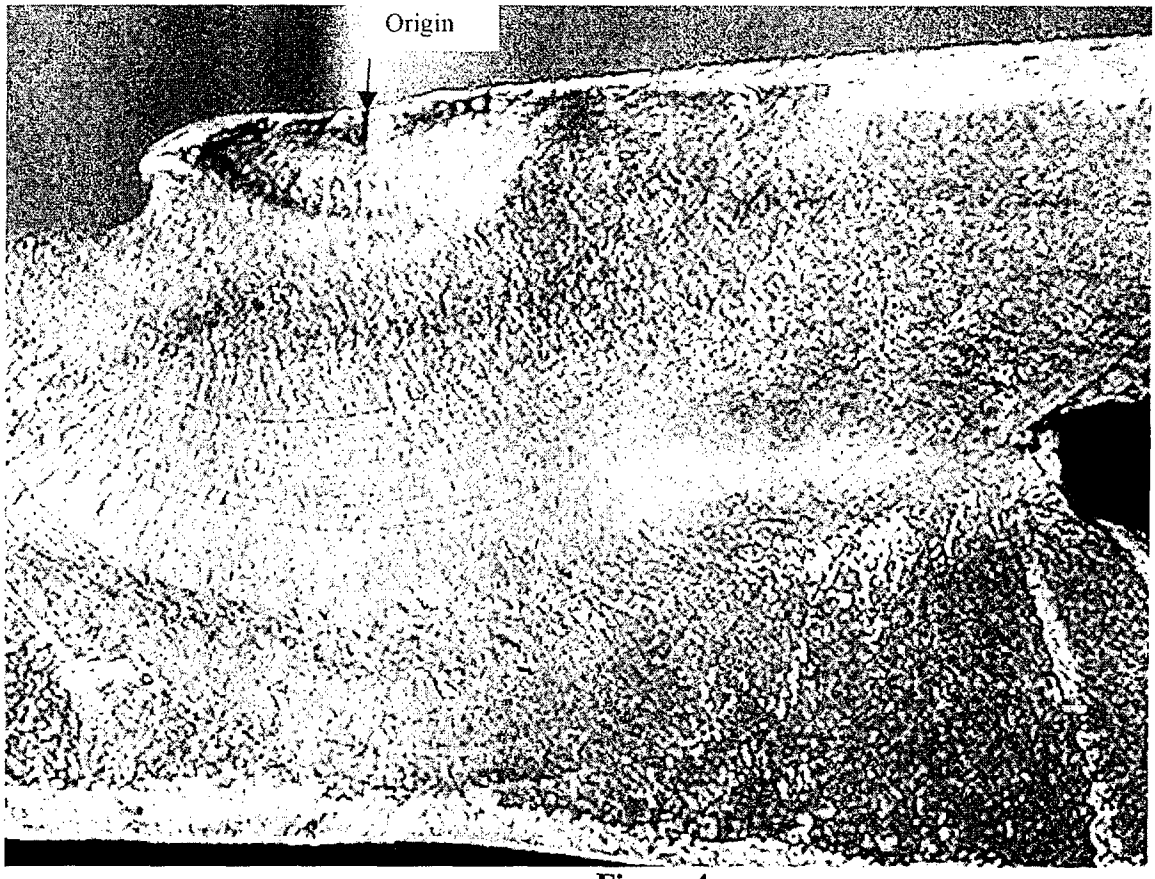

Figure 4
Fatigue Fracture Surface

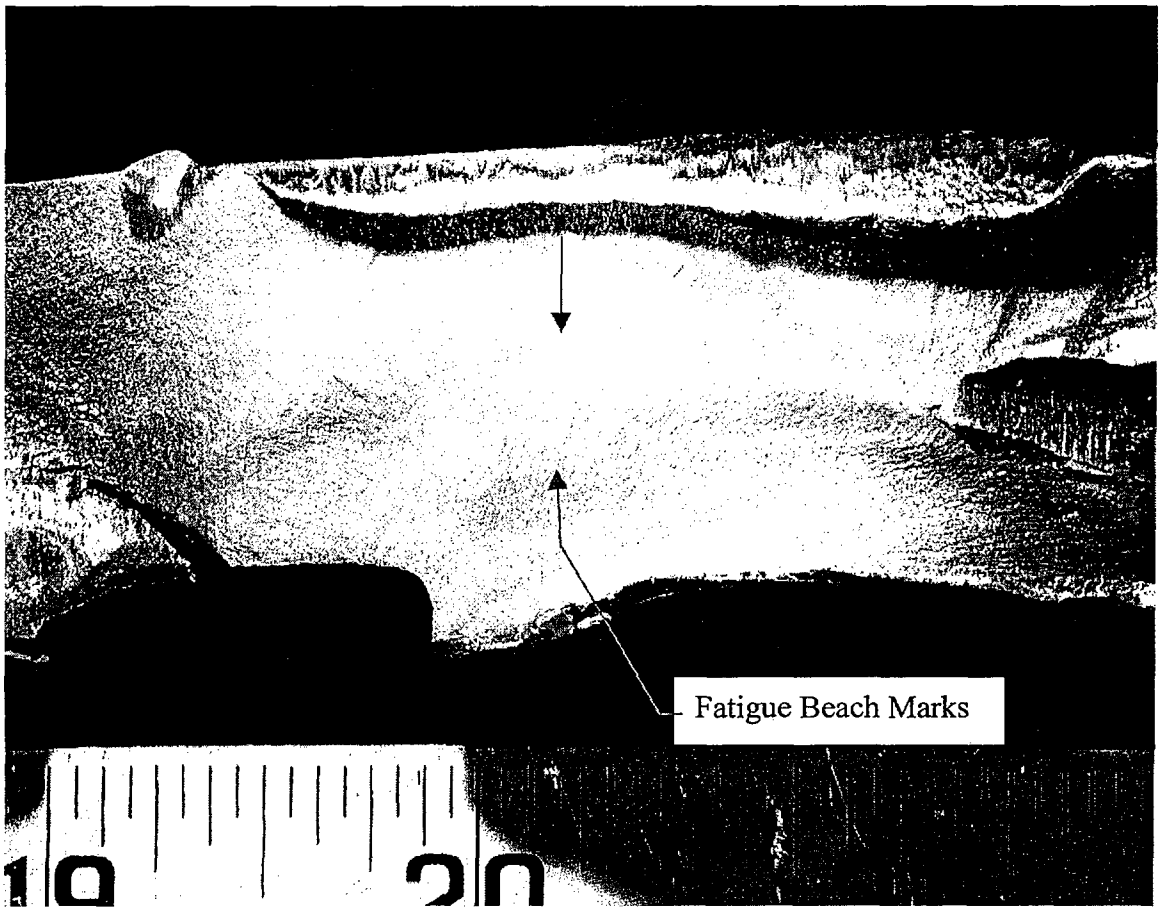

Figure 5
Fatigue Beach Marks

Figure 6
Crack Initiation and Growth Timeline
Plotted Along Engine Operating Hours

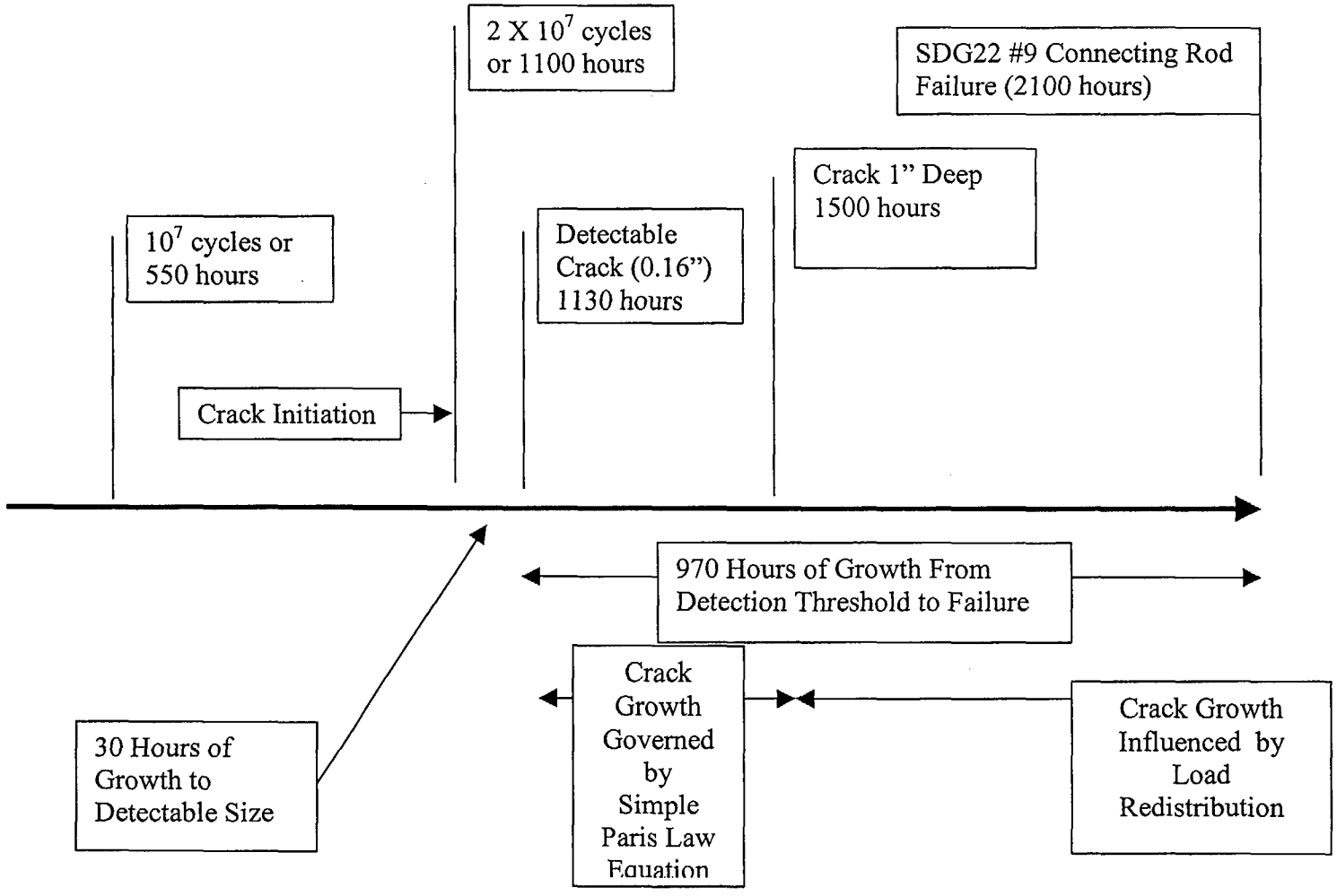

Figure 7
Schematic Representation of NDE Calibration Mockup
Not to Scale

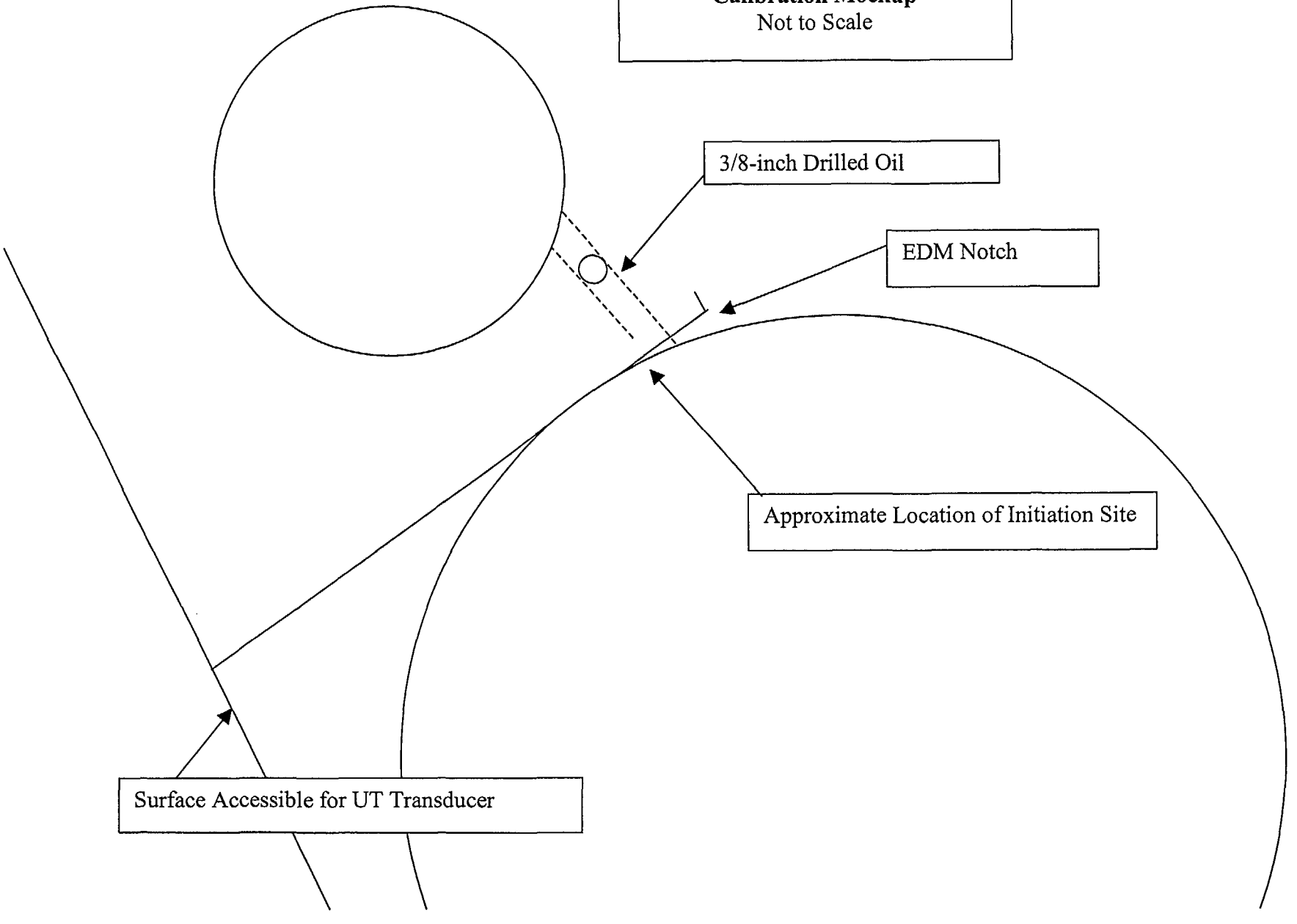

Table 1
Crack Growth Spreadsheet

Paris Law Equation, from Battelle Report, Feb 27, 1990 for actual connecting rod material

da/dN	=	$(9.77 \times 10^{-12}) \times (\Delta K)^{4.12}$
coefficient	=	9.77×10^{-12}
solve for ΔK	=	$(da/dN)^{1/4.12} / (9.77 \times 10^{-12})^{1/4.12}$
√2	=	1.414213562

18000 cycles per hour
.014 inches between beach marks at 1/2" from origin

4 hours between beach marks	1.94444×10^{-7}	$= .2 \times 10^{-6}$ inches per cycle
1/4.12 root of da/dN	0.023667914	at $da/dN = .2 \times 10^{-6}$ in./cycle,
when crack depth = 1/2 inch		
1/4.12 root of 9.77×10^{-12}	0.002127391	

		ΔK @ .2x10E-6 da/dN	da/dN =
$\Delta K = 1.94444 \times 10^{-7}/0.023667914$	at 1/2" deep	11.13	1.99849×10^{-7}
use fact that ΔK is proportional to √a , 'a' being crack depth to compute			
ΔK at 1/4 " deep		7.87	4.7927×10^{-8}
ΔK at 1/8" deep		5.56	1.14937×10^{-8}

Note: ΔK is below threshold value for crack depths less than 0.155 inches

Crack Growth Spreadsheet Data

crack depth from origin, inches	ΔK ksi sqrt(in)	da/dN inches/cycle	cycles to grow crack depth by 0.005 inches	hours to grow by 0.005 in.	Cumulative hours after ΔK >= threshold
0.15	6.1	1.67329E-08	298812	16.60	0.0
0.155	**6.2**	1.79022E-08	279295	15.52	15.5
0.16	6.3	1.91122E-08	261613	14.53	30.1
0.165	6.4	2.0363E-08	245544	13.64	43.7
0.17	6.5	2.16545E-08	230898	12.83	56.5
0.175	6.6	2.2987E-08	217514	12.08	68.6
0.18	6.7	2.43605E-08	205251	11.40	80.0
0.185	6.8	2.5775E-08	193987	10.78	90.8
0.19	6.9	2.72306E-08	183617	10.20	101.0
0.195	6.9	2.87273E-08	174050	9.67	110.7
0.2	7.0	3.02654E-08	165205	9.18	119.8

Crack Growth Spreadsheet Data

crack depth from origin, inches	ΔK ksi sqrt(in)	da/dN inches/cycle	cycles to grow crack depth by 0.005 inches	hours to grow by 0.005 in.	Cumulative hours after ΔK >= threshold
0.205	7.1	3.18447E-08	157012	8.72	128.6
0.21	7.2	3.34654E-08	149408	8.30	136.9
0.215	7.3	3.51275E-08	142339	7.91	144.8
0.22	7.4	3.68311E-08	135755	7.54	152.3
0.225	7.5	3.85763E-08	129613	7.20	159.5
0.23	7.5	4.0363E-08	123876	6.88	166.4
0.235	7.6	4.21914E-08	118508	6.58	173.0
0.24	7.7	4.40615E-08	113478	6.30	179.3
0.245	7.8	4.59734E-08	108759	6.04	185.3
0.25	7.9	4.7927E-08	104325	5.80	191.1
0.255	7.9	4.99226E-08	100155	5.56	196.7
0.26	8.0	5.196E-08	96228	5.35	202.0
0.265	8.1	5.40394E-08	92525	5.14	207.2
0.27	8.2	5.61608E-08	89030	4.95	212.1
0.275	8.3	5.83243E-08	85728	4.76	216.9
0.28	8.3	6.05299E-08	82604	4.59	221.5
0.285	8.4	6.27776E-08	79646	4.42	225.9
0.29	8.5	6.50675E-08	76843	4.27	230.2
0.295	8.5	6.73996E-08	74184	4.12	234.3
0.3	8.6	6.9774E-08	71660	3.98	238.3
0.305	8.7	7.21908E-08	69261	3.85	242.1
0.31	8.8	7.46499E-08	66979	3.72	245.8
0.315	8.8	7.71514E-08	64808	3.60	249.4
0.32	8.9	7.96954E-08	62739	3.49	252.9
0.325	9.0	8.22818E-08	60767	3.38	256.3
0.33	9.0	8.49108E-08	58885	3.27	259.6
0.335	9.1	8.75823E-08	57089	3.17	262.7
0.34	9.2	9.02965E-08	55373	3.08	265.8
0.345	9.2	9.30532E-08	53733	2.99	268.8
0.35	9.3	9.58527E-08	52163	2.90	271.7
0.355	9.4	9.86949E-08	50661	2.81	274.5
0.36	9.4	1.0158E-07	49222	2.73	277.2
0.365	9.5	1.04507E-07	47843	2.66	279.9
0.37	9.6	1.07478E-07	46521	2.58	282.5
0.375	9.6	1.10491E-07	45252	2.51	285.0
0.38	9.7	1.13548E-07	44034	2.45	287.4
0.385	9.8	1.16647E-07	42864	2.38	289.8
0.39	9.8	1.19789E-07	41740	2.32	292.1
0.395	9.9	1.22974E-07	40659	2.26	294.4

Crack Growth Spreadsheet Data

crack depth from origin, inches	ΔK ksi sqrt(in)	da/dN inches/cycle	cycles to grow crack depth by 0.005 inches	hours to grow by 0.005 in.	Cumulative hours after ΔK >= threshold
0.4	10.0	1.26202E-07	39619	2.20	296.6
0.405	10.0	1.29474E-07	38618	2.15	298.7
0.41	10.1	1.32788E-07	37654	2.09	300.8
0.415	10.1	1.36145E-07	36725	2.04	302.9
0.42	10.2	1.39546E-07	35830	1.99	304.9
0.425	10.3	1.4299E-07	34968	1.94	306.8
0.43	10.3	1.46477E-07	34135	1.90	308.7
0.435	10.4	1.50007E-07	33332	1.85	310.6
0.44	10.4	1.53581E-07	32556	1.81	312.4
0.445	10.5	1.57198E-07	31807	1.77	314.1
0.45	10.6	1.60858E-07	31083	1.73	315.9
0.455	10.6	1.64561E-07	30384	1.69	317.6
0.46	10.7	1.68308E-07	29707	1.65	319.2
0.465	10.7	1.72099E-07	29053	1.61	320.8
0.47	10.8	1.75932E-07	28420	1.58	322.4
0.475	10.8	1.7981E-07	27807	1.54	323.9
0.48	10.9	1.8373E-07	27214	1.51	325.5
0.485	11.0	1.87695E-07	26639	1.48	326.9
0.49	11.0	1.91703E-07	26082	1.45	328.4
0.495	11.1	1.95754E-07	25542	1.42	329.8
0.5	11.1	1.99849E-07	25019	1.39	331.2
0.505	11.2	2.03988E-07	24511	1.36	332.6
0.51	11.2	2.0817E-07	24019	1.33	333.9
0.515	11.3	2.12396E-07	23541	1.31	335.2
0.52	11.3	2.16666E-07	23077	1.28	336.5
0.525	11.4	2.2098E-07	22627	1.26	337.7
0.53	11.5	2.25337E-07	22189	1.23	339.0
0.535	11.5	2.29738E-07	21764	1.21	340.2
0.54	11.6	2.34183E-07	21351	1.19	341.4
0.545	11.6	2.38672E-07	20949	1.16	342.5
0.55	11.7	2.43204E-07	20559	1.14	343.7
0.555	11.7	2.47781E-07	20179	1.12	344.8
0.56	11.8	2.52401E-07	19810	1.10	345.9
0.565	11.8	2.57066E-07	19450	1.08	347.0
0.57	11.9	2.61774E-07	19100	1.06	348.0
0.575	11.9	2.66526E-07	18760	1.04	349.1
0.58	12.0	2.71322E-07	18428	1.02	350.1
0.585	12.0	2.76163E-07	18105	1.01	351.1
0.59	12.1	2.81047E-07	17791	0.99	352.1

Crack Growth Spreadsheet Data

crack depth from origin, inches	ΔK ksi sqrt(in)	da/dN inches/cycle	cycles to grow crack depth by 0.005 inches	hours to grow by 0.005 in.	Cumulative hours after ΔK >= threshold
0.595	12.1	2.85976E-07	17484	0.97	353.1
0.6	12.2	2.90948E-07	17185	0.95	354.0
0.605	12.2	2.95965E-07	16894	0.94	355.0
0.61	12.3	3.01026E-07	16610	0.92	355.9
0.615	12.3	3.06131E-07	16333	0.91	356.8
0.62	12.4	3.1128E-07	16063	0.89	357.7
0.625	12.4	3.16473E-07	15799	0.88	358.6
0.63	12.5	3.21711E-07	15542	0.86	359.4
0.635	12.5	3.26993E-07	15291	0.85	360.3
0.64	12.6	3.32319E-07	15046	0.84	361.1
0.645	12.6	3.37689E-07	14807	0.82	361.9
0.65	12.7	3.43104E-07	14573	0.81	362.7
0.655	12.7	3.48563E-07	14345	0.80	363.5
0.66	12.8	3.54066E-07	14122	0.78	364.3
0.665	12.8	3.59614E-07	13904	0.77	365.1
0.67	12.9	3.65206E-07	13691	0.76	365.9
0.675	12.9	3.70843E-07	13483	0.75	366.6
0.68	13.0	3.76524E-07	13279	0.74	367.3
0.685	13.0	3.82249E-07	13080	0.73	368.1
0.69	13.1	3.88019E-07	12886	0.72	368.8
0.695	13.1	3.93834E-07	12696	0.71	369.5
0.7	13.2	3.99693E-07	12510	0.69	370.2
0.705	13.2	4.05596E-07	12328	0.68	370.9
0.71	13.3	4.11544E-07	12149	0.67	371.5
0.715	13.3	4.17537E-07	11975	0.67	372.2
0.72	13.4	4.23574E-07	11804	0.66	372.9
0.725	13.4	4.29656E-07	11637	0.65	373.5
0.73	13.4	4.35782E-07	11474	0.64	374.1
0.735	13.5	4.41953E-07	11313	0.63	374.8
0.74	13.5	4.48169E-07	11157	0.62	375.4
0.745	13.6	4.54429E-07	11003	0.61	376.0
0.75	13.6	4.60734E-07	10852	0.60	376.6
0.755	13.7	4.67084E-07	10705	0.59	377.2
0.76	13.7	4.73478E-07	10560	0.59	377.8
0.765	13.8	4.79918E-07	10418	0.58	378.4
0.77	13.8	4.86402E-07	10280	0.57	378.9
0.775	13.9	4.9293E-07	10143	0.56	379.5
0.78	13.9	4.99504E-07	10010	0.56	380.1
0.785	13.9	5.06122E-07	9879	0.55	380.6

Crack Growth Spreadsheet Data

crack depth from origin, inches	ΔK ksi sqrt(in)	da/dN inches/cycle	cycles to grow crack depth by 0.005 inches	hours to grow by 0.005 in.	Cumulative hours after ΔK >= threshold
0.79	14.0	5.12786E-07	9751	0.54	381.2
0.795	14.0	5.19494E-07	9625	0.53	381.7
0.8	14.1	5.26247E-07	9501	0.53	382.2
0.805	14.1	5.33045E-07	9380	0.52	382.7
0.81	14.2	5.39888E-07	9261	0.51	383.2
0.815	14.2	5.46775E-07	9145	0.51	383.8
0.82	14.2	5.53708E-07	9030	0.50	384.3
0.825	14.3	5.60685E-07	8918	0.50	384.8
0.83	14.3	5.67708E-07	8807	0.49	385.2
0.835	14.4	5.74776E-07	8699	0.48	385.7
0.84	14.4	5.81888E-07	8593	0.48	386.2
0.845	14.5	5.89046E-07	8488	0.47	386.7
0.85	14.5	5.96248E-07	8386	0.47	387.1
0.855	14.5	6.03496E-07	8285	0.46	387.6
0.86	14.6	6.10789E-07	8186	0.45	388.1
0.865	14.6	6.18126E-07	8089	0.45	388.5
0.87	14.7	6.25509E-07	7993	0.44	388.9
0.875	14.7	6.32937E-07	7900	0.44	389.4
0.88	14.8	6.40411E-07	7807	0.43	389.8
0.885	14.8	6.47929E-07	7717	0.43	390.3
0.89	14.8	6.55492E-07	7628	0.42	390.7
0.895	14.9	6.63101E-07	7540	0.42	391.1
0.9	14.9	6.70755E-07	7454	0.41	391.5
0.905	15.0	6.78454E-07	7370	0.41	391.9
0.91	15.0	6.86198E-07	7287	0.40	392.3
0.915	15.1	6.93987E-07	7205	0.40	392.7
0.92	15.1	7.01822E-07	7124	0.40	393.1
0.925	15.1	7.09702E-07	7045	0.39	393.5
0.93	15.2	7.17627E-07	6967	0.39	393.9
0.935	15.2	7.25598E-07	6891	0.38	394.3
0.94	15.3	7.33614E-07	6816	0.38	394.7
0.945	15.3	7.41675E-07	6741	0.37	395.0
0.95	15.3	7.49782E-07	6669	0.37	395.4
0.955	15.4	7.57933E-07	6597	0.37	395.8
0.96	15.4	7.66131E-07	6526	0.36	396.1
0.965	15.5	7.74373E-07	6457	0.36	396.5
0.97	15.5	7.82661E-07	6388	0.35	396.8
0.975	15.5	7.90995E-07	6321	0.35	397.2
0.98	15.6	7.99374E-07	6255	0.35	397.5

Crack Growth Spreadsheet Data

crack depth from origin, inches	ΔK ksi sqrt(in)	da/dN inches/cycle	cycles to grow crack depth by 0.005 inches	hours to grow by 0.005 in.	Cumulative hours after ΔK >= threshold
0.985	15.6	8.07798E-07	6190	0.34	397.9
0.99	15.7	8.16268E-07	6125	0.34	398.2
0.995	15.7	8.24783E-07	6062	0.34	398.6
1	15.7	8.33344E-07	6000	0.33	398.9